Demonstration of a slow-light laser radar

Aaron Schweinsberg,[1,*] Zhimin Shi,[1] Joseph E. Vornehm,[1] and Robert W. Boyd[1,2]

[1]*The Institute of Optics, University of Rochester, Rochester, NY 14627, USA*
[2]*Department of Physics, University of Ottawa, Ottawa, Ontario, Canada*
*aschwei@optics.rochester.edu

Abstract: We propose and demonstrate a proof-of-concept system for a coherently combined multi-aperture slow-light laser radar. By employing slow-light delay elements in short-pulse-emitting systems to ensure synchronized pulse arrival at the target, we show that it is possible to simultaneously achieve high resolution in the transverse and the lateral dimensions with a wide steering angle.

OCIS codes: (280.3640) Lidar; (140.3298) Laser beam combining.

References and links

1. P. S. Argall and R. J. Sica, "Lidar," in *Encyclopedia of Imaging Science and Technology*, J.P. Hornak, ed. (Wiley, New York, 2002).
2. P. F. McManamon, T. A. Dorschner, D. L. Corkum, L. J. Friedman, D. S. Hobbs, M. Holz, S. Liberman, H. Q. Nguyen, D. P. Resler, R. C. Sharp, and E. A. Watson, "Optical phased array technology," Proc. IEEE **84**(2), 268–298 (1996).
3. P. F. McManamon, J. Shi, and P. K. Bos, "Broadband optical phased-array beam steering," Opt. Eng. **44**(12), 128004 (2005).
4. S. J. Augst, T. Y. Fan, and A. Sanchez, "Coherent beam combining and phase noise measurements of ytterbium fiber amplifiers," Opt. Lett. **29**(5), 474–476 (2004).
5. R. Xiao, J. Hou, M. Liu, and Z. F. Jiang, "Coherent combining technology of master oscillator power amplifier fiber arrays," Opt. Express **16**(3), 2015–2022 (2008).
6. S. Serati, H. Masterson, and A. Linnenberger, "Beam combining using a phased array of phased arrays (PAPA)," in 2004 IEEE Aerospace Conference Proceedings (IEEE, 2004), Vol. 3, 1046–1052.
7. T. M. Shay, "Theory of electronically phased coherent beam combination without a reference beam," Opt. Express **14**(25), 12188–12195 (2006).
8. T. M. Shay, V. Benham, J. T. Baker, B. Ward, A. D. Sanchez, M. A. Culpepper, D. Pilkington, J. Spring, D. J. Nelson, and C. A. Lu, "First experimental demonstration of self-synchronous phase locking of an optical array," Opt. Express **14**(25), 12015–12021 (2006).
9. I. Frigyes and A. J. Seeds, "Optically generated true-time delay in phased-array antennas," IEEE Trans. Microw. Theory **43**(9), 2378–2386 (1995).
10. S. T. Johns, D. A. Norton, C. W. Keefer, R. Erdman, and R. A. Soref, "Variable time delay of microwave signals using high dispersion fiber," Electron. Lett. **29**(6), 555–556 (1993).
11. R. D. Esman, M. Y. Frankel, J. L. Dexter, L. Goldberg, M. G. Parent, D. Stilwell, and D. G. Cooper, "Fiber-optic prism true time-delay antenna feed," IEEE Photon. Technol. Lett. **5**(11), 1347–1349 (1993).
12. M. Y. Frankel, P. J. Matthews, R. D. Esman, and L. Goldberg, "Practical optical beam forming networks," Opt. Quantum Electron. **30**(11/12), 1033–1050 (1998).
13. M. Muszkowski and E. Sędek, "Application of optical dispersion techniques in phased array antenna beam steering," J. Telecomun. Inform. Tech. **25**, C61–C64 (2008).
14. M. Bashkansky, Z. Dutton, A. Gulian, D. Walker, F. Fatemi, and M. Steiner, "True-time delay steering of phased array radars using slow light," Proc. SPIE **7226**, 72260A, 72260A-13 (2009).
15. M. Bashkansky, D. Walker, A. Gulian, and M. Steiner, "SBS-based radar true time delay," Proc. SPIE **7949**, 794918, 794918-9 (2011).
16. D. R. Walker, M. Bashkansky, A. Gulian, F. K. Fatemi, and M. Steiner, "Stabilizing slow light delay in stimulated Brillouin scattering using a Faraday rotator mirror," J. Opt. Soc. Am. B **25**(12), C61–C64 (2008).
17. F. Vasey, F. K. Reinhart, R. Houdré, and J. M. Stauffer, "Spatial optical beam steering with an AlGaAs integrated phased array," Appl. Opt. **32**(18), 3220–3232 (1993).
18. F. Xiao, W. Hu, and A. Xu, "Optical phased-array beam steering controlled by wavelength," Appl. Opt. **44**(26), 5429–5433 (2005).
19. F. Xiao, G. Li, Y. Li, and A. Xu, "Fabrication of irregular optical phased arrays on silicon-on-insulator wavers," Opt. Eng. Lett. **47**, 040503 (2008).
20. N. J. Miller, M. P. Dierking, and B. D. Duncan, "Optical sparse aperture imaging," Appl. Opt. **46**(23), 5933–5943 (2007).

21. C. R. DeHainaut, D. C. Duneman, R. C. Dymale, J. P. Blea, B. D. O'Neil, and C. E. Hines, "Wide field performance of a phased array telescope," Opt. Eng. **34**(3), 876–880 (1995).
22. T. Y. Fan, "Laser beam combining for high-power high-radiance sources," IEEE J. Sel. Top. Quantum Electron. **11**(3), 567–577 (2005).
23. J. E. Sharping, Y. Okawachi, J. van Howe, C. Xu, Y. Wang, A. E. Willner, and A. L. Gaeta, "All-optical, wavelength and bandwidth preserving, pulse delay based on parametric wavelength conversion and dispersion," Opt. Express **13**(20), 7872–7877 (2005).
24. R. Pant, M. D. Stenner, and M. A. Neifeld, "Distortion, Noise and Delay Study for Wavelength-Conversion and Dispersion Based Slow-Light System," in *Laser Science*, OSA Technical Digest (CD) (Optical Society of America, 2007), paper LWE4.
25. J. H. Abeles and R. J. Deri, "Suppression of sidelobes in the far-field radiation patterns of optical waveguide arrays," Appl. Phys. Lett. **53**(15), 1375–1377 (1988).
26. S. Yin, J. H. Kim, F. Wu, P. Ruffin, and C. Luo, "Ultra-fast speed, low grating lobe optical beam steering using unequally spaced phased array technique," Opt. Commun. **270**(1), 41–46 (2007).
27. J. A. Overbeck, M. S. Salisbury, M. B. Mark, and E. A. Watson, "Required energy for a laser radar system incorporating a fiber amplifier or an avalanche photodiode," Appl. Opt. **34**(33), 7724–7730 (1995).

1. Background

Light detection and ranging (lidar) systems have been used for many applications, including atmospheric sensing, chemical and biological agent detection, and aerial surveying [1]. Similar to radar, lidar technology offers the key advantage of improved spatial resolution because of the shorter wavelength of the radiation used. Systems that require detection over an angular range typically mount their emitting optics on a gimbal. However, coherent optical phased arrays have drawn interest for their ability to generate and sweep an optical beam without the use of large, mechanical steering elements [2,3]. In many current optical sensing systems, the large mass associated with these elements restricts the ability of the beam to steer quickly, and even where rapid steering is possible, it is generally power-intensive [2]. Phased-array steering is an alternative without these disadvantages and may also be more compatible with the aerodynamic requirements of aircraft-based sensor systems. The development of these arrays relies on several other technologies including coherent beam combining, optical phase locking, microwave phased-array beam steering, and in our case, slow light, each with their own paths of development.

Coherent combining of the output from two 10-W ytterbium-doped fiber amplifiers was accomplished by Augst *et al.*, in which the channels were phased-locked to a reference with active feedback loops using acousto-optic modulators [4]. Xiao *et al.* demonstrated coherent combination of ytterbium-doped fiber amplifiers in a 3-emitter array, using electro-optic phase modulators in each of the three fiber channels [5]. Serati *et al.* implemented side-by-side beam combining in two dimensions using a phased array of phased arrays (PAPA). In this case, phase locking was achieved via a digital loop with feedback from a camera in the far field and a liquid crystal phase control element [6]. Another method of phase control was developed and demonstrated by Shay *et al.*, who locked 9 channels with a phase accuracy of $\lambda/20$ using a technique they call LOCSET [7,8]. In LOCSET, no independent reference is required as each emitter is phase-modulated at a different frequency. The central point of the far field is imaged onto a detector and, with signal processing, the appropriate error signal is recovered and sent to a phase modulator in each channel.

Optically-induced true time delay has long been recognized to be a promising application for slow light in the field of microwave beam steering [9]. Johns *et al.* and Esman *et al.* showed that highly-dispersive optical fiber and a tunable diode laser source could be used to produce variable time delays in microwave signals for purposes of beam-steering [10,11]. Frankel *et al.* demonstrated this concept in a 4x4 array of microwave emitters, using a cascaded system with two tunable lasers where each laser controlled the beam steering in a different dimension [12]. A more recent system for incorporating optical dispersion techniques into microwave phased-array antennas was presented by Muszkowski and Sędek, who model the effect of differential channel dispersion on emitted beam direction [13]. Bashansky *et al.* have recently demonstrated that stimulated Brillouin scattering based slow light can be incorporated into the design of a phased-aperture microwave radar [14–16].

In the optical wavelength regime, beam steerers have been made based on different types of phase-shifting arrays, including liquid crystal phase shifters, and a device based on an integrated-optical array of AlGaAs waveguides with indium tin oxide/AlGaAs Shottky junctions [2,17]. Also, Xiao *et al.* have made use of a tunable source and dispersive delay to steer a beam created by a coherent array of emitting waveguides on a chip [18,19].

In the present paper, we propose and demonstrate a proof-of-concept multi-aperture laser radar system operating in the pulsed mode. In contrast to earlier systems that used optical delays to steer a microwave beam, our coherently-combined laser-radar system, which emits pulses in the optical region of the spectrum, is to the best of our knowledge, the first of its kind presented in the literature. Our system uses optical phase locking techniques to control the phase relation among multiple signal channels (sub-emitters). We also incorporate slow light to control the relative delay of pulsed signals among the channels to ensure that the emitted signals always arrive at the target simultaneously.

2. Theory/setup

There are many applications where one may wish to probe the environment via active scanning of a laser beam. In such cases, various factors will determine the longitudinal and transverse resolutions of the system. When using time-of-flight detection, the longitudinal resolution of a laser radar will be primarily limited by the duration of the emitted pulses of light, a shorter pulse giving more precise positional information. On the other hand, the transverse spatial resolution of a laser radar will be limited roughly by the focused beam size in the far field. The smallest spot to which an optical beam can be focused is roughly the diffraction-limited spot size:

$$R_{\text{far field}} = \frac{1.22 L \lambda}{D} \tag{1}$$

where λ is the wavelength, L is the distance from the emitter to the target plane and D is the diameter of the emitting aperture. We can see that the far-field transverse resolution will scale inversely with the aperture size, and therefore a large aperture is desirable. However, use of a single large aperture requires bulky opto-mechanical components for focusing and steering. Many optical sensing systems are limited in performance and cost by these beam steering and stabilizing mechanisms [2]. One method for obtaining a large effective aperture without requiring a single large emitter is to use a spaced, phased array of smaller emitters. With careful design of the sub-aperture spacing, the resolution of a multi-aperture system can be comparable to that of a single, large-aperture system [20,21].

In phased-array beam-steering, the individual phases of an array of wave-emitters need to be carefully synchronized so that the fields from different apertures will interfere in a controllable way and produce the desired transverse beam profile in the far field. In the commonly desired case of a concentrated lobe of power at a given angle, the phases are adjusted to produce constructive interference at that angle and destructive interference in other directions. Phased array technology potentially offers improvements in steering speed and removes the need for a large, moving mechanical component. If we disregard fine phase control within apertures, the situation can be considered as an N-slit diffraction pattern, which has a far-field intensity given by:

$$I(\theta) = I_0 \left(\frac{\sin(\alpha)}{\alpha} \right)^2 \left(\frac{\sin(N\beta)}{\sin(\beta)} \right)^2 \tag{2}$$

where $\alpha = (\pi a / \lambda)\sin(\theta)$, and $\beta = (\pi d / \lambda)\sin(\theta)$, with a and d representing the slit width and spacing between neighboring slits, respectively. The first sinc² factor is a broad envelope whose primary lobe width scales as λ/a. The fine fringes are defined by the second factor, and have a central lobe width proportional to the inverse of $D \equiv (N–1)d$, the total width of the

aperture array. This relationship tells us that if we want to build a scanning system with high angular resolution, we must use an appropriately wide array of emitters, bearing in mind that too low a fill fraction *a/d* will result in an unsuitably low fraction of the power going to the central lobe.

While phased-array systems have been used extensively for radio and microwave frequencies, the short wavelength of optical radiation presents special challenges. The requirement for a significant fill fraction and a tolerance to phase error at the target that may be on the order of *λ*/10 means that for large-scale devices, we are likely forced to adopt a hybrid approach [22]. Instead of having a huge number of emitters with width on the order of a wavelength, we have several large apertures, with "sub-aperture" control of the phase ramp in each element provided by a spatial light modulator, a mechanical element like a Risley prism pair or, in the case of our demonstration, simply a mirror.

Furthermore, the simultaneous requirements for good far-field transverse resolution (large *D*), good longitudinal resolution (short pulse duration *τ*), and significant steering angle *θ*, create a problem in that for wide-angle scanning, simultaneously emitted signals will arrive at the target at slightly different times and will not overlap to interfere properly. In this paper, we provide an all-optical solution for this problem by incorporating slow-light tunable delay elements into each channel. A diagram illustrating the central concept of such a system for Slow-Light Detection and Ranging (SLIDAR) is presented in Fig. 1. Pulses are carved from the output of a laser, which is then split into an array of channels. The relative path difference between the two farthest separated emitters is given by $D\sin(\theta)$. One sees that if this distance is a substantial fraction of the pulse length c/τ it becomes essential to use slow light delay elements to compensate.
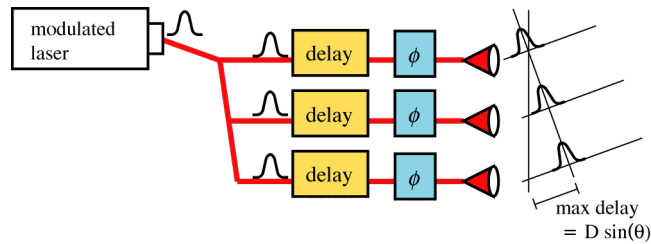

Fig. 1. Conceptual diagram of a SLIDAR system. Each channel must contain independent phase control, and group-delay control as well, if the desired steering angle is too large for a given pulse duration.

A partial schematic of our fiber-based SLIDAR experimental setup is shown in Fig. 2. A single optical reference channel is split off, and the remaining signal is pulse-carved by an intensity-modulating elecrtro-optic modulator (EOM) and divided into a number of channels leading to phased emitters. Each channel contains 1.1 km of optical fiber with different proportions of standard single-mode fiber (SMF) vs. dispersion compensating fiber (DCF) for group delay control, a phase modulating EOM with feedback to provide phase control, and an erbium-doped fiber amplifier (EDFA) running in constant-output mode before the output collimator to increase the emitted power and ensure a stable output level. Polarization controllers are needed before every electro-optic modulator to ensure that the input is linearly polarized and properly aligned relative to the EOM's fast axis. Polarization control is also needed to produce high-visibility interference patterns between the signal and reference. Half-wave plates after the output couplers of the three channels are used to ensure high-visibility interference of the free-space emission.

Our goal is to use 1–4 ns pulses in the near infrared (1550 nm) to imitate a system that observes targets at a range of over a kilometer with a full effective aperture of 1 meter. Because of space and power restrictions, our experimental target is approximately 6 meters away, with 2.1 mm diameter apertures (FWHM) and a full effective aperture of ~6.6 mm.

This setup makes the ratio between distance to the target and the effective aperture ~910:1, on the order of the ratio of 1000:1 that we are considering for a hypothetical full-scale system.

As with all phased-array systems, it is necessary to control the phase of each emitter in order to maintain the desired phase relation among different apertures. In our case, we use a heterodyne-locking scheme to phase lock every emitter to the reference that is split off before the slow-light elements. The scheme is illustrated in Fig. 2, where only a single signal channel is shown for simplicity. Each channel is independently phase-locked to the reference optical field, whose frequency is shifted by 55 MHz using an acousto-optic modulator (AOM). The reference field is split with a star coupler so that a portion of the reference can be interfered with each output channel. This optical beat signal is detected, mixed with a 55 MHz local oscillator in an RF mixer, and passed through a 1 MHz low-pass filter to give a low-frequency error signal representing the phase difference between the optical beating and the local oscillator. The error signal is input to a proportional-integral controller circuit that regulates the phase-modulating EOM and keeps the phase of the channel locked to the reference. The circuit also incorporates a "snap-back" mechanism that suddenly resets the voltage to the EOM by $2V_\pi$ when necessary to prevent a continuous ramp of phase noise from outrunning the voltage range of the phase-locking circuit. Fine control of the relative phases between the output channels is obtained by modulating low-frequency voltage signals sent to electronic phase shifters in the control circuits. Further details of the phase control scheme will be given in a future publication.
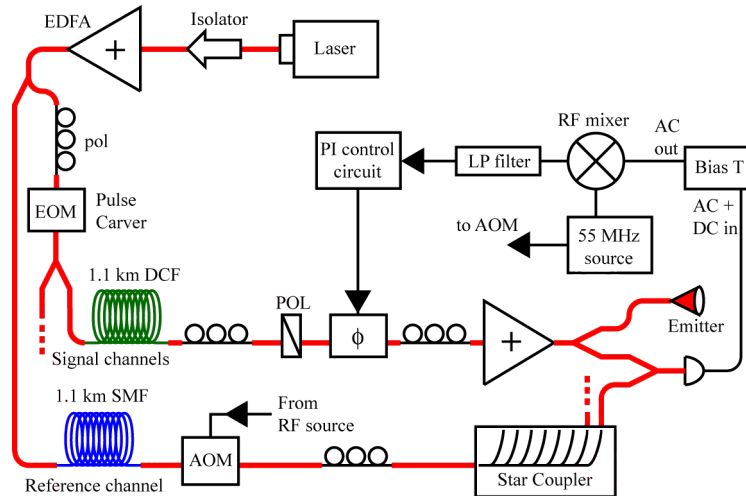

Fig. 2. Partial SLIDAR schematic, showing one channel with the reference and a block diagram of the electronic feedback path. EDFA: Erbium-doped fiber amplifier. EOM: electro-optic modulator, POL: fiber polarizer, φ: electro-optic phase modulator, AOM: acousto-optic modulator. Red lines connecting elements in the diagram represent optical fiber; black lines represent electrical connections.

Using the setup diagrammed in Fig. 2, we have successfully locked the phases of three channels, each containing a few kilometers of single-mode fiber for producing tunable slow light. Figure 3 shows the total optical power when the three output channels are combined in a fiber and allowed to interfere. The system begins with only one channel locked to the reference (i.e. no phase lock between any output channels) and the full intensity fluctuations of the phase noise can be seen. Roughly 12 seconds into data collection, a second channel is locked to the reference, and much of the intensity fluctuation vanishes. At approximately 17 seconds, the third channel is also locked, and while some jitter remains, the relative stability of the combined signal is evident.
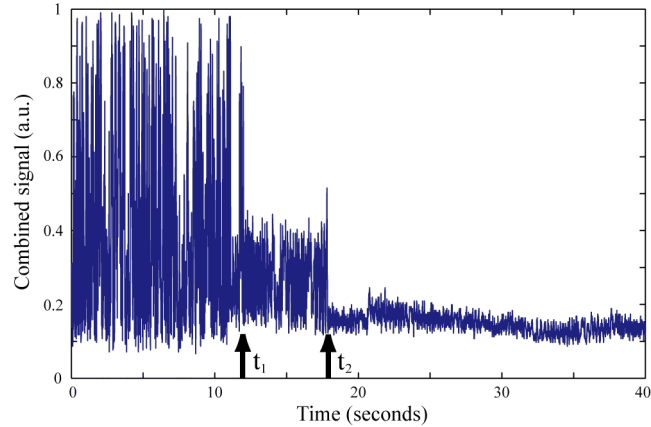
Fig. 3. SLIDAR phase locking. Starting at time t_1, two of the three channels are locked together. After time t_2, all three channels are locked.

To control the relative group delay, there are many different possible slow light technologies that could be employed. Here, we choose to use dispersive slow light, which utilizes the difference in frequency-dependent refractive index of different types of optical fiber to produce tunable relative delay by controlling the signal wavelength [23,24]. In our experiment, we use a tunable diode laser (Koshin Kogaku LS-601A) as the light source. We use standard single mode fiber as a reference medium and highly dispersive optical fiber, similar to the fiber used in telecom dispersion-compensating modules, as the slow-light medium. We have measured that a 550 m length of this fiber has a dispersion of −73 ps/nm. Each of the three channels in our SLIDAR system has approximately the same total length of fiber in each arm, but with different amounts of DCF. The relative group delay experienced by signal pulses propagating through different channels depends on the wavelength of the signal field. Figure 4 shows the relative pulse delays as functions of signal wavelength for the three channels with varying ratios of DCF to SMF. It is clear that by tuning the wavelength, we can control the relative delays of the three channels. Note that the use of a series of varying-dispersion fiber channels in this manner has also been referred to as a "fiber-optic prism" [11].
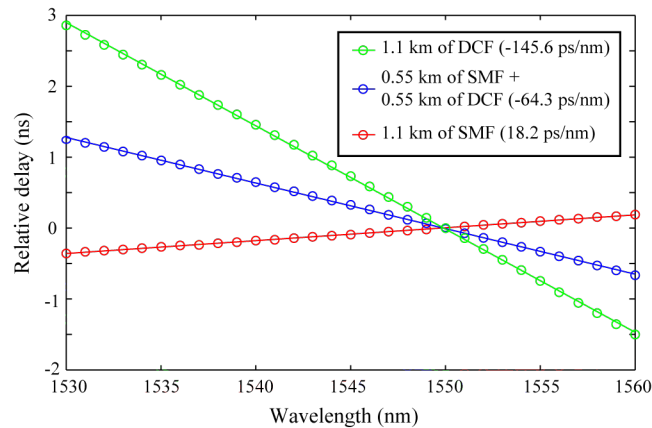

Fig. 4. Demonstration of variable dispersive delay of three SLIDAR channels. In this figure, the relative delay for each channel is set to zero at 1550 nm.

3. System tests

We have tested the SLIDAR system to show the synchronization of pulses from three channels traveling in free space, simultaneously phase-locked to a common reference. A

diagram of the setup is shown in Fig. 5. The optical signal pulses are put on a DC background so that the phase-control circuitry has a continuous signal to lock with the reference. The output pulses of the three channels are sent approximately 6 meters away where they overlap and interfere to form a far field pattern. The overlapped beam is split with a beam splitter. One part is directed onto a CCD camera to observe the transverse beam profile, while the other portion reaches the target. Because we do not have enough emitted power in our model system, we use a retro-reflecting target, rather than a scattering one. For distance resolution measurements, a delay element was placed in the target and scanned mechanically on a translation stage. For measurements of spatial resolution, a 0.44 mm slit was scanned across the beam at the target. Light retro-reflected by the target is directed back to a point near the emitters, where is collected with a lens and the signal is recorded with a 3 GHz amplified InGaAs photodetector.
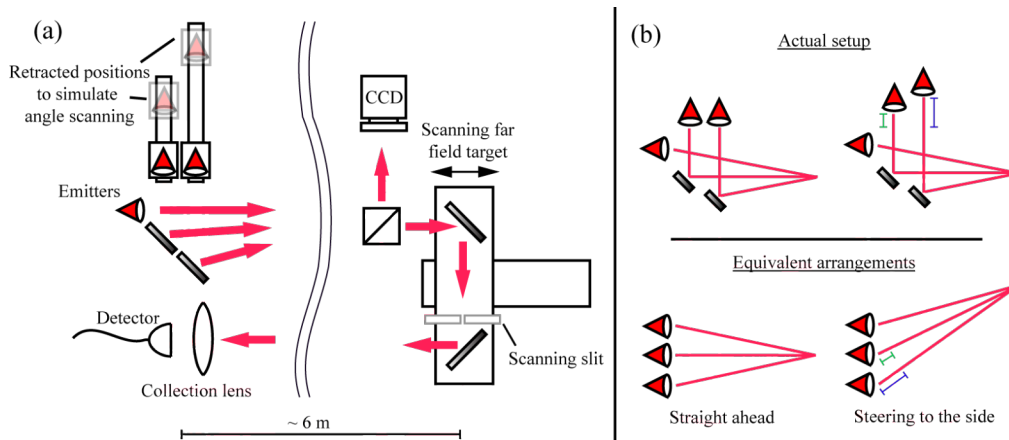

Fig. 5. (a) Setup for SLIDAR system tests. Diagram is not to scale; ~6 meters separate the emitters and the target. (b) Illustration of how translating apertures simulate side-steering of a larger scale system. The top two images represent our setup; the bottom two represent the equivalent pictures for a steered array. The green and blue bars indicate the differences in path length of light from the farther apertures.

Laboratory space and power constraints required an innovative approach to demonstrate the ability to phase-lock and synchronize a SLIDAR system with an effective aperture of one meter. In order to mimic beam steering of a full-scale system with a large aperture and long detection range, two of the output collimators were placed on translation stages. Positioning the stages close to the fixed collimator is equivalent to the situation when the beam beams are directed straight ahead, while moving the stages back is equivalent to steering the beam off-axis to one side, as illustrated in Fig. 5(b). We imitate an angular sweep of a full-scale laser radar system by moving the stages and then showing that we can resynchronize the pulses for every steering angle by controlling the wavelength of our signal field, with the beams always being phase-locked properly in each case. The results of the experiment are shown in Fig. 6.
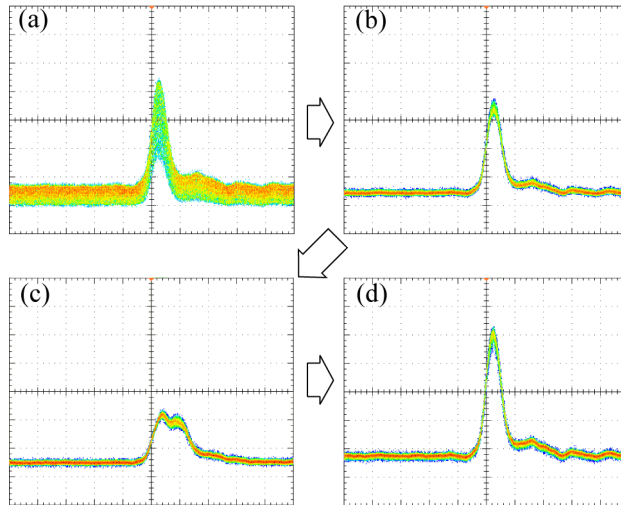
Fig. 6. Eye diagrams showing phase locking and pulse resynchronization through dispersive delay. 6(a) represents a recorded signal at 1535 nm without phase locking and with the emitters in the straight-ahead position. In going to 6(b), we have turned on the phase locking. When we shift the emitters to imitate an angular sweep, we obtain the signal seen in 6(c). Adjusting the wavelength to 1542 nm gives us the recombined signal of 6(d), showing proper synchronization and phase locking.

In Fig. 6(a), the carved pulse is shown without the phase-locking mechanism engaged. As much of the light is blocked by the slit at the target, the rapidly shifting far-field interference fringes lead to intensity fluctuations in the return signal. Here, the signal wavelength is 1535 nm. In Fig. 6(b), the locking circuits are switched on, and the intensity of the return pulse is seen to stabilize. Figure 6(c) shows what happens when we shift the emitters, showing the pulse-breakup effect that would occur when the output from a system with a one-meter full-aperture is steered 20 degrees to one side. In Fig. 6(d), the laser wavelength has been adjusted to 1542 nm which, as accurately predicted by the dispersion measurements shown in Fig. 4, was the amount needed to adjust the relative pulse delays by 1.14 ns and resynchronize the output. Despite the relative positions of the emitters, the signal can be resynchronized with a single wavelength shift because of the differing amounts of DCF in each channel. The channel with the aperture that was moved the furthest had the most dispersion (−145.6 ps/nm), while the fixed channel had the least (18.2 ps/nm).

We have also performed an experiment to measure the range-measurement accuracy of our time-of-flight SLIDAR system. As mentioned above, we mounted a retroreflector on a scanning translation stage containing at the target position. We calculated the distance to the target by measuring the return time of the emitted pulses as the stage was scanned in a series of 1 cm steps. The results are shown in Fig. 7. Fitting a line with a slope of 1.00 cm/step to the data, we find the error to have a second-order moment of only 0.38 mm. Since the stage positioning should be accurate to well under this value, this experiment demonstrates that the SLIDAR system can measure the distance to the target with very high precision.
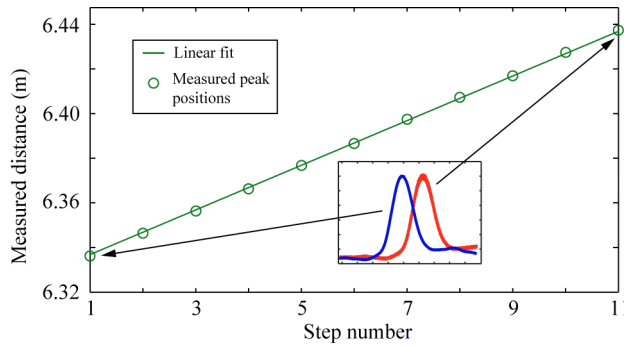
Fig. 7. Data showing tracking of an object moving away from the emitter. The inset shows the time traces of the return signal corresponding to the closest (blue) and furthest (red) positions.

By monitoring the return signal as a narrow object (in this case a slit) is moved through the beam at the target, we are able to trace out the vertically-integrated intensity pattern in the far field and estimate the spatial resolution of the SLIDAR in the scanning dimension. Traces for two different emitter configurations are shown in Fig. 8. Trace (a) shows the signal produced by two emitters having a 3.3 mm center-to-center spacing. Trace (b) shows the result if a third emitter is added, keeping the same emitter spacing and therefore increasing the total aperture to 6.6 mm. It should be possible to localize a narrow target object to within the lateral width of the SLIDAR system's central lobe of power in the far field. Comparing the results with three and two emitters, we can see that increasing the number of emitters enables us to narrow the central lobe while keeping a large fraction of the output power contained within it. In devices with more channels, it is possible to use a non-uniform spacing between emitters to reduce the peak power of the side-lobes [25,26]. By blurring the side-lobes into a more uniform pattern, interpretation of the return signal is greatly facilitated.
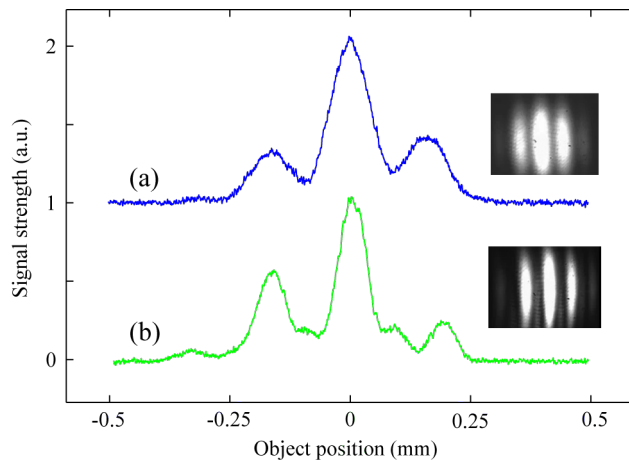

Fig. 8. Spatial resolution measurements for different beam output configurations. A slit was scanned across the far-field interference pattern of the operational SLIDAR. Trace (a) shows the return signal when two emitters are used. For trace (b), we use three emitters with the same spacing as in (a), and therefore a larger full aperture. The insets beside each data curve show the CCD image of the interference pattern. It can be seen that the addition of a third emitter allows for a narrower central lobe that still contains a high fraction of the beam's power.

4. Conclusions

We have proposed and demonstrated a proof-of-concept version of a coherently-combined multi-aperture slow-light laser radar, operating in the 1550 nm wavelength region. We have also shown that we can use dispersive delay slow-light to address the problem of mismatched pulse arrival times due to large-angle steering in one dimension. Phase control of each emitter

in our system is successfully maintained with an active-feedback phase-locking circuit. Tests of our system show good resolution in the longitudinal and transverse dimensions and suggest the feasibility of a system designed on a larger scale with many more and larger emitters. The realization of a full-scale system would require more channels, and larger, more complicated emitter structures. Combining estimates for the necessary lidar emitter pulse energy for a 20-km slant range through the atmosphere with well-known scaling laws suggests that required energies required for 1-km and 5-km remote sensing could be as low as 3.3 μJ and 81 μJ respectively under clear atmospheric conditions. Hazy atmospheric conditions would increase the required power by roughly a factor of 10 [27]. To meet these energy requirements, a full-scale system would require more powerful EDFAs at the end of each channel, as compared to the 21 dBm models in our experiment. Nonetheless, the essential enabling technologies used in our proof-of-concept system, including the techniques for optical phase locking and group delay control demonstrated here, can be transferred to a larger system in a routine fashion. While we have demonstrated a one-dimensional scanning array in the present work, it is straightforward to extend the concept to two dimensions by incorporating a second slow-light technology to create the necessary pulse delays for angle scanning in the other transverse dimension.